

Signature of the long range triplet proximity effect in the density of states

Miloš Knežević,^{1,2} Luka Trifunovic,^{1,3} and Zoran Radović¹

¹*Department of Physics, University of Belgrade, P.O. Box 368, 11001 Belgrade, Serbia*

²*Cavendish Laboratory, University of Cambridge, JJ Thomson Av., Cambridge CB3 0HE, UK*

³*Department of Physics, University of Basel, Klingelbergstrasse 82, CH-4056 Basel, Switzerland*

We study the impact of the long-range spin-triplet proximity effect on the density of states (DOS) in planar SF₁F₂S Josephson junctions that consist of conventional superconductors (S) connected by two metallic monodomain ferromagnets (F₁ and F₂) with transparent interfaces. We determine the electronic DOS in F layers and the Josephson current for arbitrary orientation of the magnetizations using the solutions of Eilenberger equations in the clean limit and for a moderate disorder in ferromagnets. We find that fully developed long-range proximity effect can occur in highly asymmetric ferromagnetic bilayer Josephson junctions with orthogonal magnetizations. The effect manifests itself as an enhancement in DOS, and as a dominant second harmonic in the Josephson current-phase relation. Distinctive variation of DOS in ferromagnets with the angle between magnetizations is experimentally observable by tunneling spectroscopy. This can provide an unambiguous signature of the long-range spin-triplet proximity effect.

PACS numbers: 74.45.+c, 74.50.+r

I. INTRODUCTION

Long-range spin-triplet superconducting correlations induced in heterostructures comprised of superconductors with the usual singlet pairing and inhomogeneous ferromagnets have been predicted recently.^{1–3} It has been experimentally verified that superconducting correlations can propagate from SF interfaces with a penetration length up to 1 μ m, and provide a nonvanishing Josephson supercurrent through very strong ferromagnets.^{4–10}

The simplest Josephson junction with inhomogeneous magnetization is SF₁F₂S structure with monodomain ferromagnetic layers having noncollinear in-plane magnetizations. However, the long-range Josephson effect is not feasible in the junctions with only two F layers,^{11–15} except in highly asymmetric SF₁F₂S junctions at low temperatures, as it was shown in Refs. 16 and 17. In that case, the long-range spin-triplet effect manifests itself as a large second harmonic ($I_2 \gg I_1$) in the expansion of the Josephson current-phase relation, $I(\phi) = I_1 \sin(\phi) + I_2 \sin(2\phi) + \dots$. The ground state in Josephson junctions with ferromagnetic barriers can be either 0 or π state. The energy of the junction is proportional to $\int_0^\phi I(\phi') d\phi'$, hence a second harmonic leads to degenerate ground states at $\phi = 0$ and $\phi = \pi$. Small contribution of the first harmonic lifts the degeneracy which results in coexistence of stable and metastable 0 and π states.¹⁸

In SFS Josephson junctions with homogeneous magnetization, the projection of the total spin of a pair to the direction of magnetization is conserved and only spin-singlet and triplet correlations with zero spin projection occur.¹⁹ These correlations penetrate into the ferromagnet over a short distance (determined by the exchange energy \hbar) $\xi_F = \hbar v_F / h$ in the clean limit and $\xi_F = \sqrt{\hbar D / h}$ in the dirty limit, where diffusion coefficient $D = v_F l / 3$. For inhomogeneous magnetization, odd-frequency triplet correlations with nonzero (± 1) total spin projection are

present as well. These correlations, not suppressed by the exchange interaction, are long-ranged, $\xi_F = \hbar v_F / k_B T (\sqrt{\hbar D / k_B T})$ in the clean (dirty) limit, and have a dramatic impact on the Josephson effect.³

Dominant influence of long-range triplet correlations on the Josephson current can be realized in SFS junctions with magnetically active interfaces,^{20,21} narrow domain walls between S and thick F interlayers with misaligned magnetizations,^{11–13,22–24} or superconductors with spin orbit interaction.²⁵ In addition to the impact on the Josephson current, the odd-frequency triplet pair correlations can be seen through enhanced electronic density of states by tunneling spectroscopy.²⁶ It has been found that proximity effect in diffusive FNS or NFS structures (N is a normal nonmagnetic metal), with magnetically active interface or precessing magnetization, gives a clearcut signature of the odd-frequency superconducting correlations.^{27,28} In general, measuring DOS is a very powerful tool to characterize the nature of superconducting correlations in NS and FS structures.^{29,30}

In this article, we study the proximity effect and influence of spin-triplet superconducting correlations in clean and moderately diffusive SF₁F₂S junctions with transparent interfaces. Magnetic interlayer is composed of two monodomain ferromagnets with arbitrary orientation of in-plane magnetizations. We calculate density of states (DOS) in ferromagnetic layers and the Josephson current from the solutions of the Eilenberger equations. Previously, F₁SF₂ and SF₁F₂S junctions with monodomain ferromagnetic layers having noncollinear in-plane magnetizations have been studied using Bogoliubov-de Gennes equation^{14,31–33} and within the quasiclassical approximation in diffusive^{15,34–40} and clean^{41,42} limits using Usadel and Eilenberger equations, respectively.

We present analytical solutions in stepwise approximation in the clean limit, and numerical self-consistently obtained results both in the clean limit and for a moderate disorder in ferromagnets. The second harmonic in the

Josephson current-phase relation is dominant for highly asymmetric SF_1F_2S junctions composed of particularly thin (weak) and thick (strong) ferromagnetic layers with noncollinear magnetizations. This is a manifestation of the long-range spin-triplet proximity effect at low temperatures, related to the phase coherent transport of two Cooper pairs.^{16,17} The proximity effect is also accompanied by pronounced change of both shape and magnitude of electronic DOS in ferromagnetic layers near the Fermi surface. In this case, the self-consistency and finite (but large) electronic mean free path do not alter the analytical results qualitatively. On the other hand, in symmetric SFFS junctions, with equal and strong magnetic influence of F layers, the long-range proximity effect is weak (cannot be dominant¹⁶); we show that DOS is therefore equal to its normal metal value even for moderately diffusive ferromagnets.

The article is organized as follows. In Sec. II, we present the model and the equations that we use to calculate the electronic DOS and the Josephson current. In Sec. III, we provide results for different ferromagnetic layers thickness and orientation of magnetizations. The conclusion is given in Sec. IV.

II. MODEL AND SOLUTIONS

We consider a simple model of an SF_1F_2S heterojunction consisting of two conventional (*s* wave, spin-singlet pairing) superconductors (S) and two uniform monodomain ferromagnetic layers (F_1 and F_2) of thickness d_1 and d_2 , with angle $\alpha = \alpha_2 - \alpha_1$ between their in-plane magnetizations (see Fig. 1). Interfaces between layers are fully transparent and magnetically inactive.

We describe superconductivity in the framework of the Eilenberger quasiclassical theory.^{3,43} Ferromagnetism is modeled by the Stoner model, using an exchange energy shift $2\hbar$ between the spin subbands. Disorder is characterized by the electron mean free path $l = v_F\tau$, where τ is the average time between scattering on impurities, and v_F is the Fermi velocity assumed to be the same in S and F metals.

Both the clean and moderately diffusive ferromagnetic layers are considered. In the clean limit, the mean free path l is larger than the two characteristic lengths: the ferromagnetic exchange length $\xi_F = \hbar v_F/\hbar$, and the superconducting coherence length $\xi_S = \hbar v_F/\pi\Delta_0$, where Δ_0 is the bulk superconducting pair potential. For moderate disorder, $\xi_F < l < \xi_S$.

In this model, the Eilenberger Green functions $g_{\sigma\sigma'}(x, \theta, \omega_n)$, $g_{\sigma\sigma'}^\dagger(x, \theta, \omega_n)$, $f_{\sigma\sigma'}(x, \theta, \omega_n)$, and $f_{\sigma\sigma'}^\dagger(x, \theta, \omega_n)$ depend on the Cooper pair center-of-mass coordinate x along the junction axis, angle θ of the quasiclassical trajectories with respect to the x axis, and on the Matsubara frequencies $\omega_n = \pi k_B T(2n + 1)$, $n = 0, \pm 1, \dots$. Spin indices are $\sigma = \uparrow, \downarrow$. The Eilenberger equation in particle-hole \otimes spin space can be written in

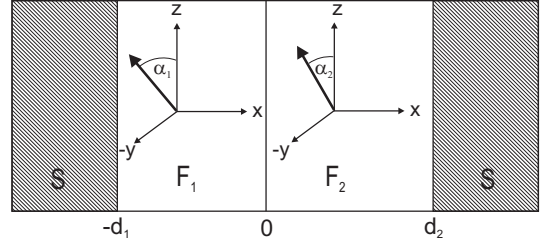


FIG. 1. Schematics of an SF_1F_2S heterojunction. The magnetization vectors lie in the y - z plane at angles α_1 and α_2 with respect to the z -axis.

the compact form

$$\hbar v_x \partial_x \tilde{g} + \left[\omega_n \hat{\tau}_3 \otimes \hat{1} - i\tilde{V} - \tilde{\Delta} + \hbar \langle \tilde{g} \rangle / 2\tau, \tilde{g} \right] = 0, \quad (1)$$

with normalization condition $\tilde{g}^2 = \hat{1}$. We indicate by $\hat{\cdot}$ and $\hat{\cdot} \cdot \hat{\cdot}$ 2×2 and 4×4 matrices, respectively. The brackets $\langle \dots \rangle = (1/2) \int_0^\pi (\dots) \sin(\theta) d\theta$ denote angular averaging over the Fermi surface, $[\ , \]$ denotes a commutator, and $v_x = v_F \cos \theta$ is the projection of the Fermi velocity vector on the x axis.

The matrix of quasiclassical Green functions is^{16,44}

$$\tilde{g} = \begin{bmatrix} g_{\uparrow\uparrow} & g_{\uparrow\downarrow} & f_{\uparrow\uparrow} & f_{\uparrow\downarrow} \\ g_{\downarrow\uparrow} & g_{\downarrow\downarrow} & f_{\downarrow\uparrow} & f_{\downarrow\downarrow} \\ -f_{\uparrow\uparrow}^\dagger & -f_{\uparrow\downarrow}^\dagger & -g_{\uparrow\uparrow}^\dagger & -g_{\uparrow\downarrow}^\dagger \\ -f_{\downarrow\uparrow}^\dagger & -f_{\downarrow\downarrow}^\dagger & -g_{\downarrow\uparrow}^\dagger & -g_{\downarrow\downarrow}^\dagger \end{bmatrix}, \quad (2)$$

and the matrix \tilde{V} is given by

$$\tilde{V} = \hat{1} \otimes \text{Re}[\mathbf{h}(x) \cdot \hat{\boldsymbol{\sigma}}] + i\hat{\tau}_3 \otimes \text{Im}[\mathbf{h}(x) \cdot \hat{\boldsymbol{\sigma}}], \quad (3)$$

where the components $\hat{\sigma}_x, \hat{\sigma}_y, \hat{\sigma}_z$ of the vector $\hat{\boldsymbol{\sigma}}$, and $\hat{\tau}_1, \hat{\tau}_2, \hat{\tau}_3$ are the Pauli matrices in the spin and the particle-hole space, respectively. The in-plane (y - z) magnetizations of the neighboring F layers are not collinear in general, and form angles α_1 and α_2 with respect to the z -axis in the left (F_1) and the right (F_2) ferromagnets. The exchange field in ferromagnetic layers is $\mathbf{h}(x) = h_1(0, \sin \alpha_1, \cos \alpha_1)$ and $h_2(0, \sin \alpha_2, \cos \alpha_2)$.

We assume that the superconductors are identical, with

$$\tilde{\Delta} = \begin{bmatrix} 0 & \hat{\sigma}_2 \Delta \\ \hat{\sigma}_2 \Delta^* & 0 \end{bmatrix} \quad (4)$$

for $x < -d_1$ and $x > d_2$. The self-consistency condition for the pair potential $\Delta = \Delta(x)$ is given by

$$\Delta = -i\lambda\pi N_0(0)k_B T \sum_{\omega_n} \langle f_{\uparrow\downarrow} \rangle, \quad (5)$$

where λ is the coupling constant, $N_0(0) = mk_F/\pi^2\hbar^2$ is the density of states (per unit volume) of the free electron gas at the Fermi level $E_F = \hbar^2 k_F^2/2m$, and $k_F = mv_F/\hbar$ is the Fermi wave number. In F layers $\tilde{\Delta} = 0$.

The density of states normalized by its normal-state value is given by analytical continuation

$$N(\varepsilon)/N_0(0) = \frac{1}{2} \sum_{\sigma} \langle \text{Re } g_{\sigma\sigma}(i\omega_n \rightarrow \varepsilon + i\delta) \rangle, \quad (6)$$

where a small imaginary part of the energy is introduced to regularize singularities. In numerical calculations we choose $\delta/\Delta_0(0) = 10^{-2}$.

The supercurrent is obtained from the normal Green function through the following expression

$$I(\phi) = \frac{1}{2} \pi e N_0(0) S k_B T \sum_{\omega_n} \sum_{\sigma} \langle v_x \text{Im } g_{\sigma\sigma} \rangle, \quad (7)$$

where ϕ is the macroscopic phase difference across the junction, and S is the area of the junction. In our examples, the current is normalized to $\pi\Delta_0/eR_N$ where $R_N = 2\pi^2\hbar/Se^2k_F^2$.

We consider only transparent interfaces and use continuity of the Green functions as the boundary conditions. Analytical solutions of Eq. (1) are derived (see Appendix) in the stepwise approximation for the pair potential

$$\Delta = \Delta_0 \left[e^{-i\phi/2} \Theta(-x - d_1) + e^{i\phi/2} \Theta(x - d_2) \right], \quad (8)$$

where Δ_0 is the bulk pair potential, and $\Theta(x)$ is the Heaviside step function. The temperature dependence of the bulk pair potential Δ_0 is given by $\Delta_0(T) = \Delta_0(0) \tanh \left(1.74 \sqrt{T_c/T - 1} \right)$.⁴⁵

We have chosen $\alpha_2 = 0$, that is $\alpha = \alpha_1$. For three characteristic values of the angle between magnetizations $\alpha = 0, \pi/2$, and π , the normal Green functions in F_2 layer are x -independent and can be written in a compact form

$$g_{\sigma\sigma}(\theta, \omega_n) = \frac{\omega_n}{\Omega_n} + \frac{\Delta_0^2}{\Omega_n} \frac{1}{\omega_n + i\Omega_n \text{sign}(\cos \theta) \cot \left(\pm \frac{\vartheta_1 + \vartheta_2}{2} + i \frac{\Xi_n}{2} - \frac{\phi}{2} \right)}, \quad (9)$$

$$g_{\sigma\sigma}(\theta, \omega_n) = \frac{\omega_n}{\Omega_n} + \frac{\Delta_0^2}{\Omega_n} \frac{\omega_n [\cos(\phi - i\Xi_n) - \cos(\vartheta_1) \cos(\vartheta_2)] - i\Omega_n \text{sign}(\cos \theta) [\pm \cos(\vartheta_1) \sin(\vartheta_2) - \sin(\phi - i\Xi_n)]}{(\Omega_n^2 + \omega_n^2) \cos(\phi - i\Xi_n) + (\Omega_n^2 - \omega_n^2) \cos(\vartheta_1) \cos(\vartheta_2) + 2i\omega_n \Omega_n \text{sign}(\cos \theta) \sin(\phi - i\Xi_n)}, \quad (10)$$

$$g_{\sigma\sigma}(\theta, \omega_n) = \frac{\omega_n}{\Omega_n} + \frac{\Delta_0^2}{\Omega_n} \frac{1}{\omega_n + i\Omega_n \text{sign}(\cos \theta) \cot \left(\pm \frac{\vartheta_2 - \vartheta_1}{2} + i \frac{\Xi_n}{2} - \frac{\phi}{2} \right)}, \quad (11)$$

respectively. Here, \pm corresponds to $\sigma = \uparrow, \downarrow$, $\Omega_n^2 = \omega_n^2 + \Delta_0^2$, $\Xi_n = 2(d_1 + d_2)\omega_n/\hbar v_F \cos \theta$ and $\vartheta_j = 2d_j \hbar_j/\hbar v_F \cos \theta$, $j = 1, 2$.

The well-known normal Green functions for $\alpha = 0$ and π are the same in F_1 and F_2 layers, Eqs. (9) and (11).^{41,46} However, for $\alpha = \pi/2$ only $\sum_{\sigma} g_{\sigma\sigma}$ is the same in F_1 and F_2 . In F_1 layer, $g_{\sigma\sigma}$ is x - and σ -dependent and cannot be expressed in a compact form.

The energy of Andreev states is determined by the poles of the Green functions. In contrast to the case of collinear magnetizations, the spin splitting of Andreev states is absent for orthogonal magnetizations, Eq. (10), where the long-range spin-triplet proximity effect is maximally pronounced.

Real part of the Green functions as a function of energy ε inside the superconducting gap, $-\Delta_0 < \varepsilon < \Delta_0$, reduces to four delta functions with θ -dependent position for collinear magnetizations, and two delta functions for orthogonal magnetizations. For planar SF_1F_2S junctions these contributions should be numerically summed over θ . Note that the electronic DOS in ferromagnets is independent of x only in the clean limit. For a finite electronic

mean free path, DOS is calculated in the middle of F_2 ferromagnetic layer.

The above results for DOS in the clean limit, obtained in the stepwise approximation for the pair potential, are not altered qualitatively in numerical self-consistent calculations. Numerical computation for both the clean limit and for moderately diffusive ferromagnets is carried out using the collocation method: Eq. (1) is solved iteratively together with the self-consistency condition, Eq. (5). Iterations are performed until self-consistency is reached, starting from the stepwise approximation for the pair potential. For a finite electron mean free path in ferromagnets, the iterative procedure starts from the clean limit. We choose the appropriate boundary conditions in superconductors at the distance exceeding $2\xi_S$ from the SF interfaces. These boundary conditions are determined by eliminating the unknown constants from the analytical solutions in stepwise approximation. To reach self-consistency with good accuracy, starting from the stepwise Δ , five to ten iterative steps were sufficient.

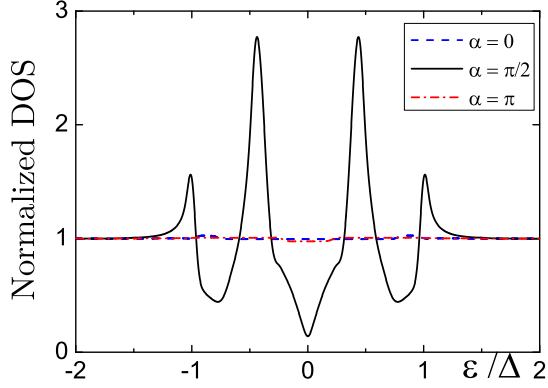


FIG. 2. (Color online) Normalized DOS, $N(\varepsilon)/N_0(0)$, in ferromagnets for an asymmetric $\text{SF}_1\text{F}_2\text{S}$ junction with $d_1 = 10k_F^{-1}$ and $d_2 = 990k_F^{-1}$, $h_1 = h_2 = 0.1E_F$. Superconductor is characterized by $\Delta_0(0)/E_F = 10^{-3}$; the phase difference $\phi = 0$. The results of non-self-consistent calculations in the clean limit, $l \rightarrow \infty$, are shown for three values of the relative angle between magnetizations: $\alpha = 0$ (dashed curve), $\pi/2$ (solid curve), and π (dash-dotted curve).

III. RESULTS

We illustrate our results on $\text{SF}_1\text{F}_2\text{S}$ planar junctions with relatively weak ferromagnets, $h/E_F = 0.1$, and the ferromagnetic exchange length $\xi_F = 20k_F^{-1}$. Superconductors are characterized by the bulk pair potential at zero temperature $\Delta_0(0)/E_F = 10^{-3}$, which corresponds to the superconducting coherence length $\xi_S(0) = 636k_F^{-1}$. We assume that all interfaces are fully transparent and the Fermi wave numbers in all metals are equal ($k_F^{-1} \sim 1\text{\AA}$).

Detailed analysis is given for a highly asymmetric junction ($d_1 = 10k_F^{-1}$ and $d_2 = 990k_F^{-1}$), Figs. 2-4, and for a symmetric junction ($d_1 = d_2 = 500k_F^{-1}$), Figs. 5 and 6. In these examples: $h_1 = h_2 = 0.1E_F$ and $T/T_c = 0.1$. In Figs. 2, 3, and 5, the results of non-self-consistent calculations for DOS and Josephson currents are shown in the clean limit ($l \rightarrow \infty$). The self-consistent numerical calculations for electronic DOS in the clean limit ($l \rightarrow \infty$) and for moderate disorder ($l = 200k_F^{-1}$) in ferromagnets are shown in Figs. 4 and 6.

In highly asymmetric $\text{SF}_1\text{F}_2\text{S}$ junctions the variation of DOS for finite electronic mean free path is less pronounced but qualitatively similar to the clean limit results, see Fig. 4. This is not the case for symmetric junctions where the long-range spin-triplet proximity effect is weak, Fig. 6.

Influence of the ferromagnet is predominantly determined by the parameter $\Theta = (h/E_F)k_F d$, and the results shown here remain the same for a large range of the junction parameters where $\Theta_1 \sim 1$ in F_1 and $\Theta_2 \sim 100$ in F_2 layers. Note that $\Theta_1 \sim 1$ is the optimal choice for

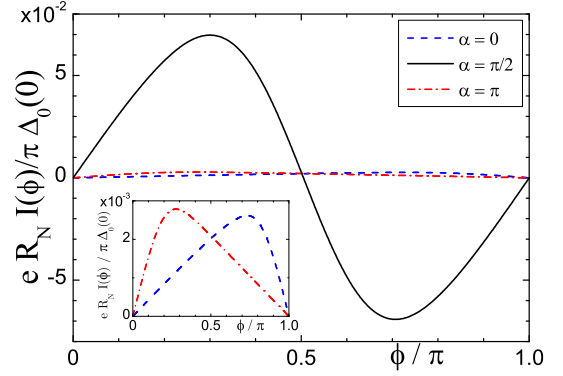


FIG. 3. (Color online) The Josephson current-phase relation $I(\phi)$ for an asymmetric $\text{SF}_1\text{F}_2\text{S}$ junction with $d_1 = 10k_F^{-1}$ and $d_2 = 990k_F^{-1}$, $h_1 = h_2 = 0.1E_F$, $l \rightarrow \infty$, $T/T_c = 0.1$, and for three values of the relative angle between magnetizations: $\alpha = 0$ (dashed curve), $\pi/2$ (solid curve), and π (dash-dotted curve). Inset: Magnified curves for $\alpha = 0$ and $\alpha = \pi$.

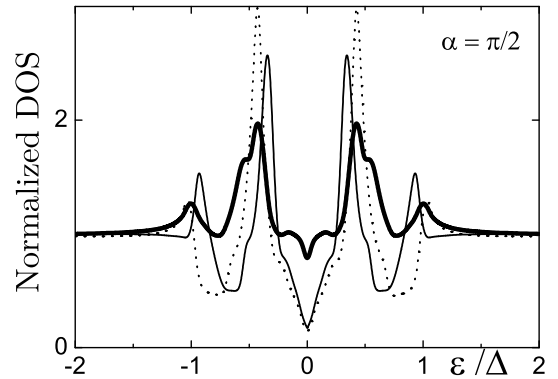


FIG. 4. Normalized DOS, $N(\varepsilon)/N_0(0)$, in ferromagnets for an asymmetric $\text{SF}_1\text{F}_2\text{S}$ junction with $d_1 = 10k_F^{-1}$ and $d_2 = 990k_F^{-1}$, $h_1 = h_2 = 0.1E_F$, for $\alpha = \pi/2$. Superconductor is characterized by $\Delta_0(0)/E_F = 10^{-3}$; the phase difference $\phi = 0$. Results of self-consistent numerical solutions in the clean limit, $l \rightarrow \infty$ (thin solid curve) and for moderately diffusive ferromagnets, $l = 200k_F^{-1}$, $x = d_2/2$ (thick solid curve) are shown. For comparison, the non-self-consistent solution in the clean limit (dotted curve) is also shown.

long-range triplet Josephson effect.²³ For experimental realization of asymmetric junctions it is more suitable to use weak and strong ferromagnets ($h_1 \ll h_2$) with small and comparable thickness ($d_1 \approx d_2$) to avoid multidomain magnetic structures and destructive influence of the orbital effect (vortices).⁴⁷

We have verified by additional calculations that the long-range triplet proximity effect in highly asymmetric $\text{SF}_1\text{F}_2\text{S}$ junctions is rather robust. Small variations in the layers thickness and in the exchange energy of

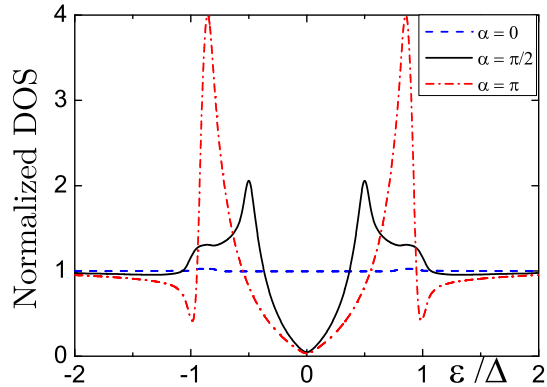


FIG. 5. (Color online) Normalized DOS, $N(\varepsilon)/N_0(0)$, in ferromagnets for a symmetric SF_1F_2S junction with $d_1 = d_2 = 500k_F^{-1}$, $h_1 = h_2 = 0.1E_F$. Superconductor is characterized by $\Delta_0(0)/E_F = 10^{-3}$; the phase difference $\phi = 0$. Results of non-self-consistent calculations in the clean limit, $l \rightarrow \infty$ are shown for three values of the relative angle between magnetizations: $\alpha = 0$ (dashed curve), $\pi/2$ (solid curve), and π (dash-dotted curve).

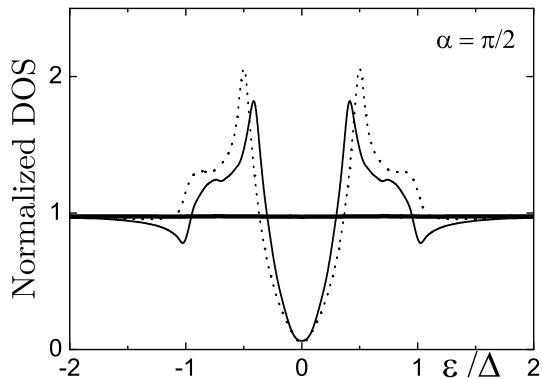


FIG. 6. Normalized DOS, $N(\varepsilon)/N_0(0)$, in ferromagnets for a symmetric SF_1F_2S junction with $d_1 = d_2 = 500k_F^{-1}$, $h_1 = h_2 = 0.1E_F$, for $\alpha = \pi/2$. Superconductor is characterized by $\Delta_0(0)/E_F = 10^{-3}$; the phase difference $\phi = 0$. Results of self-consistent numerical solutions in the clean limit, $l \rightarrow \infty$ (thin solid curve) and for moderately diffusive ferromagnets, $l = 200k_F^{-1}$, $x = d_2/2$ (thick solid curve) are shown. For comparison, the non-self-consistent solution in the clean limit (dotted curve) is also shown.

ferromagnets, as well as moderate disorder, do not affect distinctive feature of DOS. Likewise, the long-ranged second harmonic in $I(\phi)$ at low temperatures remains dominant.¹⁶

In all calculations we have assumed transparent SF interfaces and clean or moderately disordered ferromag-

nets. Finite transparency, as well as large disorder, strongly suppress the Josephson current and the electronic DOS approaches its normal state value.

In symmetric SFFS junctions with equal ferromagnetic layers no substantial impact of long-range spin-triplet superconducting correlations on the Josephson current has been found previously both in the ballistic and diffusive regimes.^{14–17} It can be seen from Figs. 5 and 6 that the electronic DOS for $\alpha = \pi/2$ is much less pronounced than for the corresponding (equal strength and total thickness of ferromagnets) asymmetric junction, Figs. 2 and 3. Moreover, for moderate disorder in ferromagnets, $l = 200k_F^{-1}$, the proximity effect is practically absent, and DOS equals its normal value (Fig. 6). In symmetric SFFS junctions the Josephson critical current monotonically increases with angle between the magnetizations, except in the vicinity of $0 - \pi$ transitions.¹⁶ In the clean limit for $\alpha = \pi$, the influence of opposite magnetizations in F layers practically cancels out and the proximity effect is much stronger, see Fig. 5. Both DOS and the Josephson current-phase relation are the same as for the corresponding SNS junction, where N stands for a normal nonmagnetic metal ($h_1 = h_2 = 0$). Recently, substantially enhanced supercurrent has been observed in Josephson junctions with ferromagnetic Fe/Cr/Fe trilayer in the antiparallel configuration, without long-range spin-triplet correlations.⁴⁸

IV. CONCLUSION

We have studied the spin-triplet proximity effect in SF_1F_2S planar junctions made of conventional superconductors and two monodomain ferromagnetic layers with arbitrary thickness, strength, and angle between in-plane magnetizations. We have derived analytical expressions for the quasiclassical normal Green functions in the clean limit and the stepwise pair potential approximation (non self-consistent). We have calculated the electronic density of states in ferromagnets, and the Josephson current. In addition, results of the numerical self-consistent calculations for the clean and moderately diffusive ferromagnets are shown for comparison.

The second harmonic in the Josephson current-phase relation is dominant for highly asymmetric SF_1F_2S junctions composed of particularly thin (weak) and thick (strong) ferromagnetic layers with noncollinear magnetizations. This is a manifestation of the long-range spin-triplet proximity effect at low temperatures, related to the phase coherent transport of two Cooper pairs. We find that the proximity effect is also accompanied by distinctive variation of electronic DOS in ferromagnetic layers as a function of energy near the Fermi surface. This variation is less pronounced in moderately diffusive case, but still detectable by tunneling spectroscopy as a signature of the long-range proximity effect. The self-consistency and finite (but large) electronic mean free path do not alter the analytical results qualitatively. In

contrast, in symmetric junctions with moderately diffusive and thick ferromagnets the long-range proximity effect is absent and DOS is equal to its normal metal value.

In summary, fully developed long-range proximity effect occurs in highly asymmetric SF_1F_2S junctions with orthogonal magnetizations. Dominant second harmonic in the Josephson current-phase relation, as well as a distinctive variation of DOS in ferromagnetic layers with the angle between magnetizations, should be experimentally observable for relatively small interface roughness and relatively clean ferromagnetic layers at low temperatures.

V. ACKNOWLEDGMENT

The work was supported by the Serbian Ministry of Science, Project No. 171027. Z. R. acknowledges Miha-jlo Vanević, Ivan Božović, and Marco Aprili for helpful discussions.

VI. APPENDIX

In the clean limit, $l \rightarrow \infty$, solutions of Eq. (1) in the step-wise approximation, Eq. (8), for the left superconductor ($x < -d_1$) can be written in the usual form for normal Green functions

$$g_{\uparrow\uparrow}(x) = \frac{\omega_n}{\Omega_n} + D_1 e^{\kappa_s x}, \quad (12)$$

$$g_{\uparrow\downarrow}(x) = D_2 e^{\kappa_s x}, \quad (13)$$

$$g_{\downarrow\uparrow}(x) = D_3 e^{\kappa_s x}, \quad (14)$$

$$g_{\downarrow\downarrow}(x) = \frac{\omega_n}{\Omega_n} + D_4 e^{\kappa_s x}, \quad (15)$$

and for anomalous Green functions

$$f_{\uparrow\uparrow}(x) = -\frac{2i\Delta_0}{2\omega_n + \hbar v_x \kappa_s} D_2 e^{\kappa_s x}, \quad (16)$$

$$f_{\uparrow\downarrow}(x) = \frac{i\Delta_0}{\Omega_n} + \frac{2i\Delta_0}{2\omega_n + \hbar v_x \kappa_s} D_1 e^{\kappa_s x}, \quad (17)$$

$$f_{\downarrow\uparrow}(x) = -\frac{i\Delta_0}{\Omega_n} - \frac{2i\Delta_0}{2\omega_n + \hbar v_x \kappa_s} D_4 e^{\kappa_s x}, \quad (18)$$

$$f_{\downarrow\downarrow}(x) = \frac{2i\Delta_0}{2\omega_n + \hbar v_x \kappa_s} D_3 e^{\kappa_s x}, \quad (19)$$

with

$$\kappa_s = \frac{2\Omega_n}{\hbar v_F |\cos(\theta)|}, \quad (20)$$

and $\Omega_n = \sqrt{\omega_n^2 + |\Delta|^2}$. For the right superconductor ($x > d_2$), the solutions retain the same form with $\kappa_s \rightarrow -\kappa_s$, $\phi \rightarrow -\phi$, with a new set of constants D'_1, \dots, D'_4 .

Solutions for the Green functions in the left ferromagnetic layer F_1 , $-d_1 < x < 0$, for three values of angle $\alpha_1 = 0, \pi/2, \pi$ (we have chosen $\alpha_2 = 0$) can be written as follows. For collinear magnetizations $\alpha_1 = 0$ and π ,

$$g_{\uparrow\uparrow}(x) = K_1, \quad (21)$$

$$g_{\uparrow\downarrow}(x) = K_2 e^{\pm i\kappa_0 x}, \quad (22)$$

$$g_{\downarrow\uparrow}(x) = K_3 e^{\mp i\kappa_0 x}, \quad (23)$$

$$g_{\downarrow\downarrow}(x) = K_4, \quad (24)$$

and

$$f_{\uparrow\uparrow}(x) = C_1 e^{i\kappa x}, \quad (25)$$

$$f_{\uparrow\downarrow}(x) = C_2 e^{i\kappa \pm x}, \quad (26)$$

$$f_{\downarrow\uparrow}(x) = C_3 e^{i\kappa \mp x}, \quad (27)$$

$$f_{\downarrow\downarrow}(x) = C_4 e^{i\kappa x}, \quad (28)$$

where the upper (lower) sign corresponds to $\alpha_1 = 0$ ($\alpha_1 = \pi$). For orthogonal magnetizations, $\alpha_1 = \pi/2$,

$$g_{\uparrow\uparrow}(x) = K_1 + K_2 e^{i\kappa_0 x} + K_3 e^{-i\kappa_0 x}, \quad (29)$$

$$g_{\uparrow\downarrow}(x) = K_4 + iK_2 e^{i\kappa_0 x} - iK_3 e^{-i\kappa_0 x}, \quad (30)$$

$$g_{\downarrow\uparrow}(x) = -K_4 + iK_2 e^{i\kappa_0 x} - iK_3 e^{-i\kappa_0 x}, \quad (31)$$

$$g_{\downarrow\downarrow}(x) = K_1 - K_2 e^{i\kappa_0 x} - K_3 e^{-i\kappa_0 x}, \quad (32)$$

and

$$f_{\uparrow\uparrow}(x) = C_1 e^{i\kappa x} + C_2 e^{i\kappa + x} + C_3 e^{i\kappa - x}, \quad (33)$$

$$f_{\uparrow\downarrow}(x) = C_4 e^{i\kappa x} - iC_2 e^{i\kappa + x} + iC_3 e^{i\kappa - x}, \quad (34)$$

$$f_{\downarrow\uparrow}(x) = C_4 e^{i\kappa x} + iC_2 e^{i\kappa + x} - iC_3 e^{i\kappa - x}, \quad (35)$$

$$f_{\downarrow\downarrow}(x) = -C_1 e^{i\kappa x} + C_2 e^{i\kappa + x} + C_3 e^{i\kappa - x}. \quad (36)$$

Here,

$$\kappa_0 = 2h_1/\hbar v_x, \quad (37)$$

$$\kappa = 2i\omega_n/\hbar v_x, \quad (38)$$

$$\kappa_{\pm} = 2(i\omega_n \pm h_1)/\hbar v_x. \quad (39)$$

For the right ferromagnetic layer F_2 , $0 < x < d_2$, $\alpha_2 = 0$, the solutions are the same as for the layer F_1 in the case $\alpha_1 = 0$, with $h_1 \rightarrow h_2$ and a new set of constants $K'_1, \dots, K'_4, C'_1, \dots, C'_4$.

The complete solution has 24 unknown coefficients: 4 + 4 in superconducting electrodes, and 8 + 8 in ferromagnetic layers. Continuity of normal and anomalous Green functions at the three interfaces provide the necessary set of 24 equations.

¹ F. S. Bergeret, A. F. Volkov, and K. B. Efetov, Phys. Rev. Lett. **86**, 4096 (2001).

² A. F. Volkov, F. S. Bergeret, and K. B. Efetov, Phys. Rev.

Lett. **90**, 117006 (2003).

³ F. S. Bergeret, A. F. Volkov, and K. B. Efetov, Rev. Mod. Phys. **77**, 1321 (2005).

- ⁴ I. Sosnin, H. Cho, V. T. Petrashov, and A. F. Volkov, *Phys. Rev. Lett.* **96**, 157002 (2006).
- ⁵ R. S. Keizer, S. T. B. Goennenwein, T. M. Klapwijk, G. Miao, G. Xiao, and A. Gupta, *Nature* **439**, 825 (2006).
- ⁶ M. S. Anwar, F. Czeschka, M. Hesselberth, M. Porcu, and J. Aarts, *Phys. Rev. B* **82**, 100501 (2010).
- ⁷ J. Wang, M. Singh, M. Tian, N. Kumar, B. Liu, C. Shi, J. K. Jain, N. Samarth, T. E. Mallouk, and M. H. W. Chan, *Nature Phys.* **6**, 389 (2010).
- ⁸ D. Sprungmann, K. Westerholt, H. Zabel, M. Weides, and H. Kohlstedt, *Phys. Rev. B* **82**, 060505(R) (2010).
- ⁹ T. S. Khaire, M. A. Khasawneh, W. P. Pratt, and N. O. Birge, *Phys. Rev. Lett.* **104**, 137002 (2010).
- ¹⁰ J. W. A. Robinson, J. D. S. Witt, and M. G. Blamire, *Science* **329**, 59 (2010).
- ¹¹ V. Braude and Y. V. Nazarov, *Phys. Rev. Lett.* **98**, 077003 (2007).
- ¹² M. Houzet and A. I. Buzdin, *Phys. Rev. B* **76**, 060504 (2007).
- ¹³ A. F. Volkov and K. B. Efetov, *Phys. Rev. B* **81**, 144522 (2010).
- ¹⁴ Z. Pajić, M. Božović, Z. Radović, J. Cayssol, and A. Buzdin, *Phys. Rev. B* **74**, 184509 (2006).
- ¹⁵ B. Crouzy, S. Tollis, and D. A. Ivanov, *Phys. Rev. B* **75**, 054503 (2007).
- ¹⁶ L. Trifunovic, Z. Popović, and Z. Radović, *Phys. Rev. B* **84**, 064511 (2011).
- ¹⁷ L. Trifunovic, *Phys. Rev. Lett.* **107**, 047001 (2011).
- ¹⁸ Z. Radović, L. Dobrosavljević-Grujić, and B. Vujić, *Phys. Rev. B* **63**, 214512 (2001).
- ¹⁹ A. I. Buzdin, *Rev. Mod. Phys.* **77**, 935 (2005).
- ²⁰ M. Eschrig, J. Kopu, J. C. Cuevas, and G. Schön, *Phys. Rev. Lett.* **90**, 137003 (2003).
- ²¹ M. Eschrig and T. Löfwander, *Nature Phys.* **4**, 138 (2008).
- ²² A. F. Volkov and K. B. Efetov, *Phys. Rev. B* **78**, 024519 (2008).
- ²³ L. Trifunovic and Z. Radović, *Phys. Rev. B* **82**, 020505 (2010).
- ²⁴ M. Alidoust and J. Linder, *Phys. Rev. B* **82**, 224504 (2010).
- ²⁵ M. Duckheim and P. W. Brouwer, *Phys. Rev. B* **83**, 054513 (2011).
- ²⁶ A. Cottet, *Phys. Rev. Lett.* **107**, 177001 (2011).
- ²⁷ T. Yokoyama, Y. Tanaka, and A. A. Golubov, *Phys. Rev. B* **75**, 134510 (2007).
- ²⁸ T. Yokoyama and Y. Tserkovnyak, *Phys. Rev. B* **80**, 104416 (2009).
- ²⁹ S. Pilgram, W. Belzig, and C. Bruder, *Phys. Rev. B* **62**, 12462 (2000).
- ³⁰ F. Pérez-Willard, J. C. Cuevas, C. Sürgers, P. Pfundstein, J. Kopu, M. Eschrig, and H. v. Löhneysen, *Phys. Rev. B* **69**, 140502 (2004).
- ³¹ Y. Asano, Y. Tanaka, and A. A. Golubov, *Phys. Rev. Lett.* **98**, 107002 (2007).
- ³² K. Halterman, P. H. Barsic, and O. T. Valls, *Phys. Rev. Lett.* **99**, 127002 (2007).
- ³³ K. Halterman, O. T. Valls, and P. H. Barsic, *Phys. Rev. B* **77**, 174511 (2008).
- ³⁴ Y. Fominov, A. Golubov, and M. Kupriyanov, *JETP Lett.* **77**, 510 (2003).
- ³⁵ C. You, Y. B. Bazaliy, J. Y. Gu, S. Oh, L. M. Litvak, and S. D. Bader, *Phys. Rev. B* **70**, 014505 (2004).
- ³⁶ T. Löfwander, T. Champel, J. Durst, and M. Eschrig, *Phys. Rev. Lett.* **95**, 187003 (2005).
- ³⁷ Y. S. Barash, I. V. Bobkova, and T. Kopp, *Phys. Rev. B* **66**, 140503 (2002).
- ³⁸ Y. V. Fominov, A. F. Volkov, and K. B. Efetov, *Phys. Rev. B* **75**, 104509 (2007).
- ³⁹ I. B. Sperstad, J. Linder, and A. Sudbø, *Phys. Rev. B* **78**, 104509 (2008).
- ⁴⁰ T. Y. Karinskaya, A. A. Golubov, M. Y. Kupriyanov, and A. S. Sidorenko, *Phys. Rev. B* **79**, 214509 (2009).
- ⁴¹ Y. M. Blanter and F. W. J. Hekking, *Phys. Rev. B* **69**, 024525 (2004).
- ⁴² J. Linder, M. Zareyan, and A. Sudbø, *Phys. Rev. B* **79**, 064514 (2009).
- ⁴³ G. Eilenberger, *Z. Phys.* **190**, 142 (1966).
- ⁴⁴ Our matrix \tilde{g} and Eq. (1) are equivalent up to a unitary transformation to the definitions used in Ref. 3.
- ⁴⁵ B. Mühlischlegel, *Z. Phys.* **155**, 313 (1959).
- ⁴⁶ F. Konschelle, J. Cayssol, and A. I. Buzdin, *Phys. Rev. B* **78**, 134505 (2008).
- ⁴⁷ I. F. Lyuksyutov and V. L. Pokrovsky, *Adv. Phys.* **54**, 67 (2005).
- ⁴⁸ J. W. A. Robinson, G. B. Halász, A. I. Buzdin, and M. G. Blamire, *Phys. Rev. Lett.* **104**, 207001 (2010).